ANALYTICAL SOLUTIONS OF SUPERDIRECTIVITY FOR CIRCULAR ARRAYS WITH ACOUSTIC VECTOR SENSORS

Yong Wang[a], Yixin Yang[b], Yuanliang Ma[b], Bing Li[a]

[a]No.28, Xianning West Road, Xi'an, Shaanxi, 710049, P. R. China
[b]No. 127, West Youyi Road, Xi'an, Shaanxi, 710072, P. R. China

Contact author: Yong Wang, School of Mechanical Engineering, Xi'an Jiaotong University, No.28, Xianning West Road, Xi'an, Shaanxi, 710049, P. R. China, yongwang.nwpu@gmail.com

Abstract: *Sensor arrays with superdirectivity are more attractive than conventional sensor arrays in many applications such as sonar, radar, and audio engineering, because they have good performance in terms of angular discrimination, bearing estimation accuracy, and noise suppression ability with a relatively much smaller aperture. A superdirectivity theory termed the eigenbeam decomposition and synthesis theory has been previously proposed for circular pressure sensor arrays. This paper applies this theory in circular vector sensor arrays, which aims to achieving better performance than both superdirective pressure sensor arrays and conventional vector sensor arrays. For simplicity, each sensor of the circular arrays considered only consists of one pressure channel and one particle velocity channel. It is found that the optimal beampattern, global optimum directivity factor, and total error sensitivity function can be accurately expressed as the sum of eigenbeams, sum of their directivity factors, and sum of their sensitivity functions, respectively, with the use of the circulant property of the spatial cross-correlation matrix and the inverse of block matrix. Because the robustness of different eigenbeams are different, a reduced-order technique similar to that proposed for circular pressure sensor arrays can also be used to achieve robust superdirectivity for circular vector sensor arrays. The comparisons between circular pressure sensor arrays with circular vector sensor arrays show that the capability of the latter arrays in improving directivity is better than that of the former arrays.*

Keywords: *Superdirectivity, circular array, vector sensor, optimal beamforming*

1. INTRODUCTION

Pressure sensors and acoustic vector sensors (AVSs) are often used in many acoustic applications to capture signals. The former sensors sense the acoustic scalar pressure and have an omnidirectional directivity pattern in free-field, whereas the latter ones pick up the acoustic pressure and vectorial particle velocity components at a single point in space simultaneously and usually have a frequency-independent directivity by combining pressure and acoustic particle velocity channels in a single package. Unlike pressure sensor arrays, AVSs and their arrays have just taken quick development in recent years [1]. In comparison with pressure sensor arrays, AVS arrays have some different properties and can improve performance in terms of signal enhancement, bearing estimation, and noise suppression, et al., and thus have been received more and more attention recently.

Gur presented a mode beamforming method for small linear velocity sensor arrays [1]. Guo et al. studied the low-frequency mode beamforming for a small rectangular AVS array [2] and derived an upper bound of the directivity index (DI) [3]. Wang et al. [4] analysed the array gain of a conformal AVS array in a practical environment using the optimization-based beamforming method. Moreover, Yang et al. studied the direction-of-arrival estimation for a circular AVS array that is mounted on a cylindrical baffle [5].

Recently, the superdirectivity of circular pressure sensor arrays have been studied in detail and the theoretical closed-form solutions were derived based on the eigenbeam decomposition and synthesis (EBDS) theory [6-8]. Actually, the similar theoretical closed-form solutions of superdirectivity also exist for circular AVS arrays, which are derived in this paper. The obtained solutions for circular AVS arrays show some different properties from those of the circular pressure sensor arrays. Simulations are provided to evaluate the performance of the proposed method.

2. SIGNAL MODEL

The circular array considered contains M uniformly spaced vector sensors, and each vector sensor only consists of one pressure channel and one particle velocity channel for simplicity, as shown in Fig.1. The particle velocity channels are all put along the radial direction or the tangential direction. The radius of the circular array is a. A unit-magnitude plane wave impinges from direction (θ,ϕ), where θ and ϕ denote the elevation and azimuth angles, respectively. The pressure received by the mth AVS at the spherical coordinate of $(a,\phi_m,\pi/2)$ is $p_m(\theta,\phi)=\exp[ika\sin\theta\cos(\phi-\phi_m)]$, where $i=\sqrt{-1}$, the wavenumber is $k=2\pi/\lambda$, and λ denotes the wavelength. The acoustic particle velocity components received by the mth AVS are derived as

$$v_{r,m}(\theta,\phi)=\frac{\partial p_m}{\partial r}\Big|_{r=a}=V_r\sin\theta\cos(\phi-\phi_m)\exp[ika\sin\theta\cos(\phi-\phi_m)] \quad \text{(radial orientation)}, \tag{1}$$

$$v_{\phi,m}(\theta,\phi)=\frac{\partial p_m}{\partial \phi}\Big|_{r=a}=-V_\phi\sin\theta\sin(\phi-\phi_m)\exp[ika\sin\theta\cos(\phi-\phi_m)] \quad \text{(tangential orientation)}, \tag{2}$$

where $\phi_m=m\beta$, $\beta=2\pi/M$, V_r and V_ϕ are the amplitudes of the velocity measurements and they can be normalized in practice to be $V_r=V_\phi=1$. The time dependent part

$\exp(i\omega t)$, where ω is the angular frequency, has been omitted for simplicity. The manifold vector will be $\mathbf{V}_{\hbar}(\theta,\phi)=[v_{\hbar,0}(\theta,\phi),v_{\hbar,1}(\theta,\phi),\ldots,v_{\hbar,M-1}(\theta,\phi)]^T$, where $\hbar$ can be replaced by r or ϕ, the superscript T indicates the transpose. The manifold vector for circular AVS arrays will be $\mathbf{M}=[\mathbf{P}^T,\mathbf{V}_{\hbar}^T]^T$, where $\mathbf{P}(\theta,\phi)=[p_0(\theta,\phi),\ldots,p_{M-1}(\theta,\phi)]^T$.

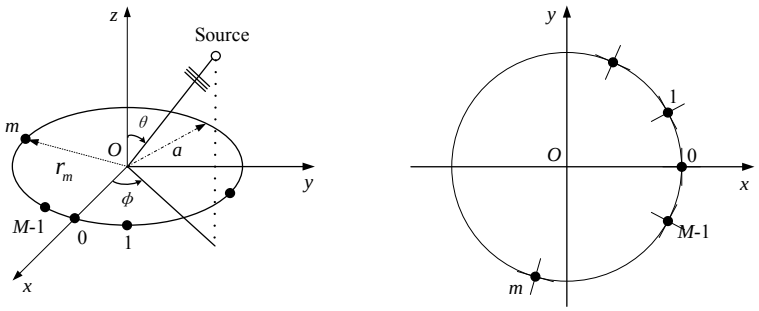

(a) Coordinates. *(b) Top view.*

Fig. 1: Circular vector sensor array. The black point denotes the AVS and the cross on it marks the main response axes of the two particle velocity channels.

The beampattern describes the sensitivity of a beamformer to a plane wave impinging on the array from direction (θ,ϕ), which is defined as

$$B(\theta_0,\phi_0,\theta,\phi)=\mathbf{w}^H(\theta_0,\phi_0)\mathbf{M}(\theta,\phi), \tag{3}$$

where the superscript H indicates the Hermitian transpose, the vector $\mathbf{w}$ is the weighting vector, and (θ_0,ϕ_0) is the pre-set steering direction.

The optimal weighting vector to achieve the maximum directivity factor (DF) is $\mathbf{w}_{\text{opt}}=\alpha\boldsymbol{\rho}^{-1}\mathbf{P}(\theta_0,\phi_0)$ [7, 8], where $\alpha=1/[\mathbf{P}^H(\theta_0,\phi_0)\boldsymbol{\rho}^{-1}\mathbf{P}(\theta_0,\phi_0)]$ and the maximum directivity factor (DF) is equal to $1/\alpha$ and directivity index (DI) is $DI=10\log DF$. The matrix $\boldsymbol{\rho}$ is the normalized spatial cross-correlation matrix of the circular AVS array, which is defined as $\boldsymbol{\rho}=(4\pi)^{-1}\int_0^{2\pi}\int_0^{\pi}\mathbf{M}(\theta,\phi)\mathbf{M}^H(\theta,\phi)\sin\theta d\theta d\phi$. The error sensitivity function (SF) of the beamforming method is defined as $SF=\|\mathbf{w}\|^2$ and sensitivity index (SI) is $SI=10\log SF$ [7, 8], which is always used to evaluate the robustness of the beamforming method.

The matrix $\boldsymbol{\rho}$ can be written as $\boldsymbol{\rho}=\begin{bmatrix}\boldsymbol{\rho}_{pp} & \boldsymbol{\rho}_{p\hbar}\\ \boldsymbol{\rho}_{\hbar p} & \boldsymbol{\rho}_{\hbar\hbar}\end{bmatrix}_{2M\times 2M}$, where $\boldsymbol{\rho}_{pp}$ is the normalized spatial cross-correlation matrix of the pressure channels, $\boldsymbol{\rho}_{\hbar\hbar}$ are the normalized spatial cross-correlation matrices of the particle velocity channels, and $\boldsymbol{\rho}_{p\hbar}$ and $\boldsymbol{\rho}_{\hbar p}$ are the normalized spatial cross-correlation matrices between the pressure and particle velocity channels.

By virtue of the related conclusions in [9], it can be obtained that

$$\rho_{rr,m_1m_2}=\rho_{rr,s}=(kd)^{-1}j_1(kd)\cos(s\beta)+j_2(kd)a^2d^{-2}[1-\cos(s\beta)]^2, \tag{4}$$

$$\rho_{\phi\phi,m_1m_2}=\rho_{\phi\phi,s}=(kd)^{-1}j_1(kd)\cos(s\beta)-j_2(kd)a^2d^{-2}\sin(s\beta)^2, \tag{5}$$

$$\rho_{pr,m_1m_2}=\rho_{pr,s}=-ij_1(kd)ad^{-1}[1-\cos(s\beta)]=-\rho_{rp,m_1m_2}=-\rho_{rp,s}, \tag{6}$$

$$\rho_{p\phi,m_1m_2}=\rho_{p\phi,s}=ij_1(kd)ad^{-1}\sin(s\beta)=\rho_{\phi p,m_1m_2}=\rho_{\phi p,s}, \tag{7}$$

where d is the spacing between two AVSs, $s=|m_1-m_2|$, $j_n(\cdot)$ is the nth-order spherical Bessel function of the first kind.

The inverse matrix of $\boldsymbol{\rho}$ is $\boldsymbol{\rho}^{-1}=\begin{bmatrix}\tilde{\boldsymbol{\rho}}_{pp}^{-1} & \tilde{\boldsymbol{\rho}}_{p\hbar}^{-1}\\ \tilde{\boldsymbol{\rho}}_{\hbar p}^{-1} & \tilde{\boldsymbol{\rho}}_{\hbar\hbar}^{-1}\end{bmatrix}$, where $\tilde{\boldsymbol{\rho}}_{pp}^{-1}=\boldsymbol{\rho}_{pp}^{-1}+\boldsymbol{\rho}_{pp}^{-1}\boldsymbol{\rho}_{p\hbar}\mathbf{Q}^{-1}\boldsymbol{\rho}_{\hbar p}\boldsymbol{\rho}_{pp}^{-1}$, $\tilde{\boldsymbol{\rho}}_{p\hbar}^{-1}=-\boldsymbol{\rho}_{pp}^{-1}\boldsymbol{\rho}_{p\hbar}\mathbf{Q}^{-1}$, $\tilde{\boldsymbol{\rho}}_{\hbar p}^{-1}=-\mathbf{Q}^{-1}\boldsymbol{\rho}_{\hbar p}\boldsymbol{\rho}_{pp}^{-1}$, $\tilde{\boldsymbol{\rho}}_{\hbar\hbar}^{-1}=\mathbf{Q}^{-1}$, $\mathbf{Q}=\boldsymbol{\rho}_{\hbar\hbar}-\boldsymbol{\rho}_{\hbar p}\boldsymbol{\rho}_{pp}^{-1}\boldsymbol{\rho}_{p\hbar}$. It is easily proved that $\boldsymbol{\rho}_{pp}$, $\boldsymbol{\rho}_{\hbar\hbar}$, $\boldsymbol{\rho}_{p\hbar}$, $\boldsymbol{\rho}_{\hbar p}$, $\tilde{\boldsymbol{\rho}}_{pp}$, $\tilde{\boldsymbol{\rho}}_{p\hbar}$, $\tilde{\boldsymbol{\rho}}_{\hbar p}$, and $\tilde{\boldsymbol{\rho}}_{\hbar\hbar}$ are all circulant matrix and their eigenvectors are $\mathbf{v}_m=M^{-1/2}[1,e^{im\beta},\ldots,e^{i(M-1)m\beta}]^T$ [10]. The eigenvalues of $\boldsymbol{\rho}_{pp}$, $\boldsymbol{\rho}_{\hbar\hbar}$, $\boldsymbol{\rho}_{p\hbar}$, and $\boldsymbol{\rho}_{\hbar p}$ can be expressed as $\lambda_{\hbar\lambda,m}=\sum_{s=0}^{M-1}\rho_{\hbar\lambda,s}e^{ism\beta}$, where ($\hbar,\lambda=p,r,\phi$). The eigenvalues of $\tilde{\boldsymbol{\rho}}_{pp}^{-1}$, $\tilde{\boldsymbol{\rho}}_{p\hbar}^{-1}$, $\tilde{\boldsymbol{\rho}}_{\hbar p}^{-1}$, and $\tilde{\boldsymbol{\rho}}_{\hbar\hbar}^{-1}$ are derived as

$$\frac{1}{\tilde{\lambda}_{pp,m}}=\frac{\lambda_{\hbar\hbar,m}}{\lambda_{pp,m}\lambda_{\hbar\hbar,m}-|\lambda_{p\hbar,m}|^2},\quad \frac{1}{\tilde{\lambda}_{p\hbar,m}}=\frac{1}{\tilde{\lambda}_{\hbar p,m}^*}=-\frac{\lambda_{p\hbar,m}}{\lambda_{pp,m}\lambda_{\hbar\hbar,m}-|\lambda_{p\hbar,m}|^2},$$
$$\frac{1}{\tilde{\lambda}_{\hbar\hbar,m}}=\frac{1}{\lambda_{Q,m}}=\frac{\lambda_{pp,m}}{\lambda_{pp,m}\lambda_{\hbar\hbar,m}-|\lambda_{p\hbar,m}|^2}, \tag{8}$$

respectively.

Inserting the expression of $\boldsymbol{\rho}^{-1}$ into $\mathbf{w}_{\text{opt}}=\alpha\boldsymbol{\rho}^{-1}\mathbf{P}(\theta_0,\phi_0)$ yields

$$\mathbf{w}_{\text{opt}}=\alpha\begin{bmatrix}\tilde{\boldsymbol{\rho}}_{pp}^{-1} & \tilde{\boldsymbol{\rho}}_{p\hbar}^{-1}\\ \tilde{\boldsymbol{\rho}}_{\hbar p}^{-1} & \tilde{\boldsymbol{\rho}}_{\hbar\hbar}^{-1}\end{bmatrix}\begin{bmatrix}\mathbf{P}(\theta_0,\phi_0)\\ \mathbf{V}_\hbar(\theta_0,\phi_0)\end{bmatrix}=\alpha\begin{bmatrix}\tilde{\boldsymbol{\rho}}_{pp}^{-1}\mathbf{P}(\theta_0,\phi_0)+\tilde{\boldsymbol{\rho}}_{p\hbar}^{-1}\mathbf{V}_\hbar(\theta_0,\phi_0)\\ \tilde{\boldsymbol{\rho}}_{\hbar p}^{-1}\mathbf{P}(\theta_0,\phi_0)+\tilde{\boldsymbol{\rho}}_{\hbar\hbar}^{-1}\mathbf{V}_\hbar(\theta_0,\phi_0)\end{bmatrix}=\alpha\begin{bmatrix}\sum_{m=0}^{M-1}\left(\frac{1}{\tilde{\lambda}_{pp,m}}\mathbf{v}_m\mathbf{v}_m^H\right)\mathbf{P}(\theta_0,\phi_0)+\left(\frac{1}{\tilde{\lambda}_{p\hbar,m}}\mathbf{v}_m\mathbf{v}_m^H\right)\mathbf{V}_\hbar(\theta_0,\phi_0)\\ \sum_{m=0}^{M-1}\left(\frac{1}{\tilde{\lambda}_{\hbar p,m}}\mathbf{v}_m\mathbf{v}_m^H\right)\mathbf{P}(\theta_0,\phi_0)+\left(\frac{1}{\tilde{\lambda}_{\hbar\hbar,m}}\mathbf{v}_m\mathbf{v}_m^H\right)\mathbf{V}_\hbar(\theta_0,\phi_0)\end{bmatrix}. \tag{9}$$

The optimal beampattern, the maximum DF, and the total SF can be derived as

$$B_{\text{opt}}(\theta,\phi)=\alpha\sum_{m=0}^{M-1}\underbrace{\left[\left(\frac{1}{\tilde{\lambda}_{pp,m}}E_{p,m}^*(\theta_0,\phi_0)+\frac{1}{\tilde{\lambda}_{p\hbar,m}^*}E_{\hbar,m}^*(\theta_0,\phi_0)\right)E_{p,m}(\theta,\phi)+\left(\frac{1}{\tilde{\lambda}_{\hbar p,m}^*}E_{p,m}^*(\theta_0,\phi_0)+\frac{1}{\tilde{\lambda}_{\hbar\hbar,m}}E_{\hbar,m}^*(\theta_0,\phi_0)\right)E_{\hbar,m}(\theta,\phi)\right]}_{\hat{B}_m(\theta,\phi)}, \tag{10}$$

$$DF_{\max}=\sum_{m=0}^{M-1}\underbrace{\left[\frac{1}{\tilde{\lambda}_{pp,m}}|E_{p,m}(\theta_0,\phi_0)|^2+\frac{1}{\tilde{\lambda}_{\hbar\hbar,m}}|E_{\hbar,m}(\theta_0,\phi_0)|^2+2\,\text{Re}\left\{\frac{1}{\tilde{\lambda}_{p\hbar,m}^*}E_{\hbar,m}^*(\theta_0,\phi_0)E_{p,m}(\theta_0,\phi_0)\right\}\right]}_{\hat{D}_m}, \tag{11}$$

$$SF_{tot}=\alpha^2\sum_{m=0}^{M-1}\underbrace{\left[\begin{array}{l}\left(\frac{1}{|\tilde{\lambda}_{pp,m}|^2}+\frac{1}{|\tilde{\lambda}_{\hbar p,m}|^2}\right)|E_{p,m}(\theta_0,\phi_0)|^2+\left(\frac{1}{|\tilde{\lambda}_{p\hbar,m}|^2}+\frac{1}{|\tilde{\lambda}_{\hbar\hbar,m}|^2}\right)|E_{\hbar,m}(\theta_0,\phi_0)|^2\\ +2\,\text{Re}\left\{\left(\frac{1}{\tilde{\lambda}_{pp,m}^*\tilde{\lambda}_{p\hbar,m}}+\frac{1}{\tilde{\lambda}_{\hbar p,m}^*\tilde{\lambda}_{\hbar\hbar,m}}\right)E_{p,m}^*(\theta_0,\phi_0)E_{\hbar,m}(\theta_0,\phi_0)\right\}\end{array}\right]}_{\hat{T}_m}, \tag{12}$$

respectively, where $E_{p,m}(\theta,\phi)=\mathbf{v}_m^H\mathbf{P}(\theta,\phi)=M^{-1/2}\sum_{s=0}^{M-1}e^{-ism\beta}\cdot p_s(\theta,\phi)$, $E_{\hbar,m}(\theta,\phi)=\mathbf{v}_m^H\mathbf{V}_\hbar(\theta,\phi)=M^{-1/2}\sum_{s=0}^{M-1}e^{-ism\beta}\cdot v_{\hbar,s}(\theta,\phi)$.

It is readily demonstrated that $\hat{B}_m=\hat{B}_{M-m}^*$, $\hat{D}_m=\hat{D}_{M-m}$, and $\hat{T}_m=\hat{T}_{M-m}$ when M is even. Thus, the optimal beampattern, the maximum DF, and the total SF under these conditions can be simplified to

$$B_{\text{opt}}(\theta,\phi)=\alpha\sum_{m=0}^{M/2}B_m(\theta,\phi)=\alpha\sum_{m=0}^{M/2}\varepsilon_m\,\text{Re}\left[\left(\begin{array}{l}\frac{1}{\tilde{\lambda}_{pp,m}}E_{p,m}^*(\theta_0,\phi_0)+\\ \frac{1}{\tilde{\lambda}_{p\hbar,m}^*}E_{\hbar,m}^*(\theta_0,\phi_0)\end{array}\right)E_{p,m}(\theta,\phi)+\left(\begin{array}{l}\frac{1}{\tilde{\lambda}_{\hbar p,m}^*}E_{p,m}^*(\theta_0,\phi_0)\\ +\frac{1}{\tilde{\lambda}_{\hbar\hbar,m}}E_{\hbar,m}^*(\theta_0,\phi_0)\end{array}\right)E_{\hbar,m}(\theta,\phi)\right], \tag{13}$$

$$DF_{\max}=\sum_{m=0}^{M/2}D_m=\sum_{m=0}^{M/2}\varepsilon_m\left[\frac{1}{\tilde{\lambda}_{pp,m}}|E_{p,m}(\theta_0,\phi_0)|^2+\frac{1}{\tilde{\lambda}_{\hbar\hbar,m}}|E_{\hbar,m}(\theta_0,\phi_0)|^2+2\,\text{Re}\left\{\frac{1}{\tilde{\lambda}_{p\hbar,m}^*}E_{\hbar,m}^*(\theta_0,\phi_0)E_{p,m}(\theta_0,\phi_0)\right\}\right], \tag{14}$$

$$SF_{tot}=\alpha^2\sum_{m=0}^{M/2}T_m=\alpha^2\sum_{m=0}^{M/2}\varepsilon_m\left[\begin{array}{l}\left(\dfrac{1}{\left|\tilde{\lambda}_{pp,m}\right|^2}+\dfrac{1}{\left|\tilde{\lambda}_{hp,m}\right|^2}\right)\left|E_{p,m}(\theta_0,\phi_0)\right|^2+\left(\dfrac{1}{\left|\tilde{\lambda}_{ph,m}\right|^2}+\dfrac{1}{\left|\tilde{\lambda}_{hh,m}\right|^2}\right)\left|E_{h,m}(\theta_0,\phi_0)\right|^2\\ +2\,\mathrm{Re}\left\{\left(\dfrac{1}{\tilde{\lambda}^*_{pp,m}\tilde{\lambda}_{ph,m}}+\dfrac{1}{\tilde{\lambda}^*_{hp,m}\tilde{\lambda}_{hh,m}}\right)E^*_{p,m}(\theta_0,\phi_0)E_{h,m}(\theta_0,\phi_0)\right\}\end{array}\right], \tag{15}$$

respectively, where $\varepsilon_m=1$ for $m=0,M/2$, and $\varepsilon_m=2$ for $m=1,\ldots,M/2-1$.

Some simulations will be provided in the following sections to further show the performance of the above-proposed method.

3. SIMULATIONS

Consider a 6-element circular AVS array and each AVS consists of a pressure channel and a radial-oriented particle velocity channel. The pre-set steering direction is $(\theta_0,\phi_0)=(\pi/2,\pi)$. The speed of sound is 1500 m/s. The DFs, SFs of different eigenbeams as well as synthesized beampatterns are shown in Fig. 2.

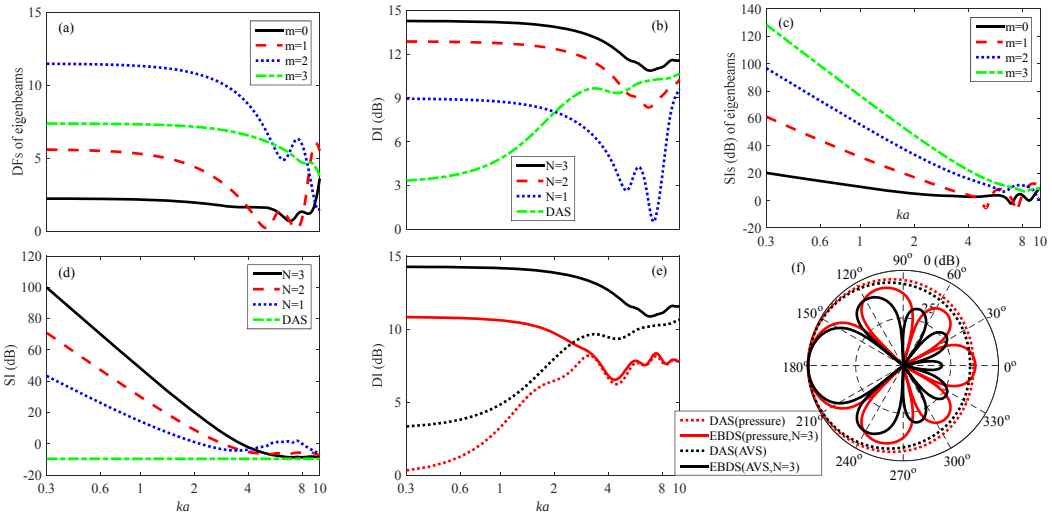

Fig. 2: Simulations for circular AVS arrays. (a) DFs of different eigenbeams. (b) DIs. (c) SFs of different eigenbeams. (d) SIs. (e) DI comparison. (f) Synthesized beampatterns.

In the high-frequency range shown in Fig. 2(a), each DF line is undulate, whereas in the low-frequency range, the DFs of eigenbeams increase with an increase in the order except for that of the 3rd-order eigenbeam, which is different from those for circular pressure sensor arrays with a single ring shown in [7, 8]. Since the total DI is the summation of the DFs of the selected eigenbeams with orders from 0 to *N*, their properties of changing with the frequency are similar, see Fig. 2(b). In Fig. 2(c), the SFs will not tend to any limit values as the frequency decreases to 0, not similar to the DFs in Fig. 2(a). Since SFs increase with the decreasing frequency, the robustness will be worse when the frequency is lower, see Fig. 2(c) and Fig. 2(d). The SFs increase with an increase in the order and it is true for all eigenbeams. Therefore, the reduced-order technique proposed in [6, 7], can also be used here to give better robustness by sacrificing some DF. As shown in Fig. 2(e), both DIs of DAS and EBDS methods for circular AVS arrays are larger than those of circular pressure sensor arrays, and the DI improvement achieved by the EBDS method is apparently greater than that of the DAS method. The beampatterns shown in Fig. 2(f) also demonstrate the above conclusions.

4. CONCLUSION

This paper proposes theoretical solutions of superdirectivity for circular AVS arrays based on the EBDS theory. The optimal beampattern, the maximum DF, and the total SF are analytically expressed as the sum of eigenbeams, sum of their DFs, and sum of their SFs, respectively, by virtue of the block matrix inverse theorem and properties of circulant matrix. The eigenbeams show different robustness, and the previously proposed reduced-order technique can also be used to achieve robust superdirectivity for circular AVS arrays. Superdirective beampatterns are obtained in simulations, which show that the capability of circular AVS arrays in improving directivity is better than that of circular pressure sensor arrays.

5. ACKNOWLEDGEMENTS

This work was supported in part by the National Natural Science Foundation of China under Grant 11604259 and in part by the China Postdoctoral Science Foundation under Grant 2016M592782.

REFERENCES

[1] **B. Gur**, Particle velocity gradient based acoustic mode beamforming for short linear vector sensor arrays, *J. Acoust. Soc. Am.*, volume (135), pp. 3463-3473, 2014.

[2] **X. J. Guo, S. e. Yang, and S. Miron**, Low-frequency beamforming for a miniaturized aperture three-by-three uniform rectangular array of acoustic vector sensors, *J. Acoust. Soc. Am.*, volume (138), pp. 3873-3883, 2015.

[3] **X. J. Guo, S. Miron, Y. X. Yang *et al.***, An upper bound for the directivity index of superdirective acoustic vector sensor arrays, *J. Acoust. Soc. Am.*, volume (140), pp. EL410-EL415, 2016.

[4] **Y. Wang, Y. X. Yang, Z.-Y. He *et al.***, Array gain for a conformal acoustic vector sensor array: An experimental study, *Chin. Phys. B* volume (25), pp. 124318, 2016.

[5] **D. Yang and Z. Zhu**, Direction-of-arrival estimation for a uniform circular acoustic vector-sensor array mounted around a cylindrical baffle, *Sci. China-Phys. Mech. Astron.*, volume (55), pp. 2338-2346, 2012.

[6] **Y. L. Ma, Y. X. Yang, Z. Y. He *et al.***, Theoretical and practical solutions for high-order superdirectivity of circular sensor arrays, *IEEE Trans. Ind. Electron.*, volume (60), pp. 203-209, 2013.

[7] **Y. Wang, Y. X. Yang, Y. L. Ma *et al.***, Robust high-order superdirectivity of circular sensor arrays, *J. Acoust. Soc. Am.*, volume (136), pp. 1712-1724, 2014.

[8] **Y. Wang, Y. X. Yang, Y. L. Ma *et al.***, High-order superdirectivity of circular sensor arrays mounted on baffles, *Acta Acust. united Ac.*, volume (102), pp. 80-93, 2016.

[9] **M. Hawkes and A. Nehorai**, Acoustic vector-sensor correlations in ambient noise, *IEEE J. Oceanic Eng.*, volume (26), pp. 337-347, 2001.

[10] **G. J. Tee**, Eigenvectors of block circulant and alternating circulant matrices, *Research Letters in the Information and Mathematical Sciences*, volume (8), pp. 123-142, 2005.